ORIGINAL ARTICLE

Sludge-based activated carbon experiment design, char properties, and evaluation of methyl orange adsorption

Ming Zhao[1] · Donghua Ji[2] · Gang Wu[1]

Abstract
Paper mill sludge is a type of industrial waste that, if improperly disposed of, can cause significant environmental pollution and resource wastage. This study aims to utilize paper mill sludge (as feedstock) and agricultural waste peanut shells (as a carburizer) to produce sludge-based activated carbon for the adsorption of dye wastewater. Orthogonal experiments were conducted to compare the adsorption properties of activated carbon prepared through physical, chemical, and microwave activation methods. The resulting activated carbon samples were then characterized using BET, SEM, XRD, and FTIR analyses. Additionally, the adsorption properties of methyl orange on the optimized activated carbon were investigated under various influencing factors, and the adsorption kinetics were studied. The findings revealed that the activated carbon prepared through chemical activation exhibited the highest performance, with an iodine adsorption value of 913.86 mg/g and a methylene blue adsorption value of 153 mg/g. BET, SEM, and FTIR analyses demonstrated that the chemically activated carbon possessed a larger specific surface area, a more developed pore structure, and a higher presence of oxygen-containing functional groups on its surface. XRD analysis indicated the presence of quartz-phase Si in the activated carbon, suggesting a higher degree of graphitization in the activated samples. The adsorption equilibrium time of optimum activated carbon for methyl orange solution was 120 min. At a solution pH of 7, the removal efficiency and adsorption capacity of methyl orange reached their highest values of 86.37% and 215.93 mg/g, respectively. Furthermore, as the activated carbon dose increased, the removal efficiency of methyl orange significantly increased while the adsorption capacity decreased. When the solution concentration reached 500 mg/L, the adsorption capacity gradually reached saturation. The adsorption kinetic behavior was better described by the quasi-second-order kinetic equation, with a high fit degree ($R^2 > 0.999$). The fit degree was high during the external diffusion stage but poor during the internal diffusion stage. These results provide valuable insights for the development of activated carbon with enhanced adsorption performance for wastewater treatment.

Keywords Activated carbon · Orthogonal experiment · Sludge · Methyl orange adsorption · Chemical activation

Highlights
- Two kinds of waste, sludge and peanut shell, were used for resource utilization.
- Physical, chemical, and microwave activation were used to prepare activated carbon.
- The orthogonal experiment was used to obtain the optimal preparation process.
- The adsorption properties, kinetics, and mechanism of methyl orange were investigated.

✉ Ming Zhao
zhaoming@seu.edu.cn

1 Key Laboratory of Energy Thermal Conversion and Control of Ministry of Education, School of Energy and Environment, Southeast University, Nanjing 210096, China

2 Japhl Powertrain Systems Co., Ltd, Nanjing 210000, China

1 Introduction

Paper mill sludge is a by-product of the paper industry, containing various pathogenic microorganisms, organic matter, nitrogen, and phosphorus. This composition poses a risk of environmental pollution and public health issues [1, 2]. The China Paper Association reports that China's paper production in 2022 reached approximately 283.91 Mt, representing a 1.32% increase compared to the previous year [3]. It is estimated that for every ton of paper produced, an average of 1 m^3 of paper sludge is generated [4]. Currently, the annual output of paper mill sludge is substantial, and commonly used disposal methods include discarding, landfilling, and incineration. However, these methods fail to achieve sludge reduction or prevent the occurrence of secondary pollution

[5]. Similarly, dye wastewater (such as methyl orange) is a common pollutant in the dye processing industry [6]. It is characterized by its complex tissue composition, high chroma, and poor biodegradation performance. The global usage of dye exceeds 10,000 t/year, with approximately 100 t entering the environment through water supply, posing risks to both humans and the environment [7]. Given the negative impacts of paper mill sludge and dye wastewater, it is crucial to explore environmentally friendly technologies to address these issues [8]. Consequently, the utilization of sludge-based activated carbon for resource recovery and environmental protection has been proposed. With its excellent porosity, sludge-based activated carbon can serve as an adsorbent carrier for dye wastewater.

Compared with biochar, sludge-based activated carbon has lower carbon content and a less developed specific surface, which limits its industrial application [9, 10]. To overcome this limitation, researchers have explored the addition of substances with high carbon content, such as lignocellulose, to sludge precursors [8, 11]. For instance, Wang et al. [12] incorporated biomass into the sludge and observed an improvement in the pore structure, with a maximum BET surface area of 1342 m^2/g after chemical treatment, leading to enhanced adsorption performance. Similarly, Liang et al. [13] demonstrated that the addition of biomass to sludge improved the physicochemical properties, particularly in the field of adsorbents. In another study, Li et al. added 25 wt.% corn stalk to the sludge and observed an increase in the specific surface area of sludge-based activated carbon from 475 to 769 m^2/g, which was advantageous for adsorption [8]. These findings highlight the significant improvement in adsorption capacity achieved by using lignocellulosic materials, such as rice husk, coconut shell, and peanut shell, as the carburizer in sludge-based activated carbon.

The physicochemical properties and adsorption performances of sludge-based activated carbon are influenced by various factors, including the proportion of sludge and carburizer, activation method, and activation conditions such as heating rate, temperature, time, and activator. Nielsen et al. [14] found that adding fish waste to the sludge increased the pore volume and specific surface area of the activated carbon by 1.5 times and 3 times, respectively, resulting in enhanced adsorption of dyes. Dos Reis et al. [15] determined that the optimal specific surface area (S_{BET}) was achieved at a pyrolysis temperature of 500 ℃, impregnation ratio of 0.5 (ZnCl$_2$-to-sludge), and holding time of 15 min. Tay et al. [16] investigated the preparation process of sludge-derived adsorbents using ZnCl$_2$ as an activator, considering factors such as concentration, activation temperature, and residence time. Their results showed that a low concentration of ZnCl$_2$ increased the proportion of micropores in the activated carbon. Activation temperature and residence time also affected the specific surface area and pore size distribution of the

activated carbon. It is important to note that the specific surface area and adsorption capacity of activated carbon can vary significantly depending on the raw materials and preparation methods used. Furthermore, many activated carbon experiments lack a comprehensive consideration of different preparation conditions. Therefore, it is crucial to conduct further research and make meaningful attempts to synthesize low-cost and high-performance activated carbon from waste.

In this study, sludge and peanut shells (as a carburizer) were chosen as the raw materials for producing activated carbon. The optimal activated carbon process was determined through an orthogonal experiment involving three activation modes: physical, chemical, and microwave activation. The resulting activated carbon was then characterized and analyzed. Subsequently, the optimal activated carbon was used for adsorbing dye wastewater (specifically, methyl orange), and the adsorption kinetics were calculated to investigate the underlying adsorption mechanism. These endeavors are crucial for advancing the utilization of sludge resources and mitigating the adverse impacts of dye wastewater.

2 Materials and methods

2.1 Materials and equipment

Paper mill sludge, purchased from Shandong Chenming Paper Co., Ltd., and peanut shells, produced in Ningling County, Shangqiu City, Henan Province, were used as raw materials. The raw materials were first purified and then dried naturally in a cool, dark place. The dried samples were crushed using a grinder and sieved into 80 mesh (particle size ~ 0.2 mm). Subsequently, the samples were further dried in a 105 °C oven for 24 h and stored in sealed bags. Zinc chloride (analytical pure) and methyl orange (analytical pure) were obtained from Nanjing Chemical Reagent Co., Ltd. for the experiment.

The test equipment included a horizontal tube furnace (YG-120810, Shanghai Yuzhi Co., Ltd.), UV–visible spectrophotometer (UV1800, Shanghai Jinghua Technology Instrument Co., Ltd.), and microwave chemical reactor (WBFY-205, Zhengzhou Yiheng Instrument Equipment Co., Ltd.).

Based on physical activation, chemical activation, and microwave activation methods, the corresponding optimal activated carbons were determined using orthogonal experiments and named AC-P$_{max}$, AC-C$_{max}$, and AC-M$_{max}$, respectively. To compare samples without physical, chemical, and microwave activation, activated carbon was prepared by directly carbonizing raw materials (sludge 70 wt.% and peanut shell 30 wt.%) under a N$_2$ atmosphere with a nitrogen flow rate of 300 mL/min, heating rate of 10 °C/min, carbonization temperature of 500 °C, and time of 60 min.

This comparison group was named AC-Raw. AC stands for activated carbon, and ACs include AC-Raw, AC-P$_{max}$, AC-C$_{max}$, and AC-M$_{max}$.

2.2 Preparation of activated carbon

This study focused on three main methods for preparing activated carbon: physical activation, chemical activation, and microwave activation. The paper mill sludge-peanut shell mixture (hereafter referred to as mixture) was obtained by adding peanut shells into paper mill sludge at proportions of 10%, 20%, and 30%.

(1) *Physical activation*. Physical activation consists of two stages: pyrolysis and activation. In the pyrolysis stage, a mixture with different mass fractions of 5 g was weighed into the tube furnace. Nitrogen gas (purity, 99.999%) was used as the protective gas at a flow rate of 300 mL/min. The mixture was then heated to 600 °C at a rate of 10 °C/min and carbonized for 60 min. In the activation stage, the carbonized sample was heated to the activation temperature (700, 800, 900 °C) using different heating rates (10, 20, 30 °C/min). Once the activation temperature was reached, the nitrogen gas was switched to high-purity CO_2 (flow rate 300 mL/min) for activation, and a specific activation time (30, 60, 90 min) was maintained. The effects of heating rate, peanut shell content, activation temperature, and activation time on the properties of activated carbon were investigated.

(2) *Chemical activation*. A 5 g mixture consisting of different mass fractions was weighed and then mixed with a specific amount of zinc chloride impregnation. The mixture was subsequently dried in an oven at 105 °C. Next, the mixture was placed in a tube furnace under a nitrogen atmosphere with a flow rate of 300 mL/min. The heating rate was set at 10 °C/min, and the mixture was heated to different activation temperatures (500, 550, 600 °C) for 30, 60, or 90 min. The resulting activated carbon was thoroughly washed with distilled water to eliminate the activator and other inorganic ash. Finally, the activated carbon was dried in the oven at 105 °C and sealed for future use.

(3) *Microwave activation*. A 5 g mixture with varying mass fractions was weighed, impregnated, and mixed with a specific mass of zinc chloride. The mixture was stirred thoroughly and left to sit for 12 h before being dried and utilized. Next, the mixture was placed into a microwave chemical reactor and subjected to microwave irradiation at power levels of 300, 500, and 700 W for durations of 10, 20, and 30 min, respectively. The resulting activated carbon was then washed multiple times with distilled water to remove any remaining activator and

inorganic ash. Finally, the activated carbon was dried and sealed.

2.3 Orthogonal experimental design

The specific surface area and adsorption properties of activated carbon were influenced by heating rate, microwave power, activation temperature, and impregnation ratio [17, 18]. To account for the numerous influencing factors, an orthogonal experimental design was employed, which allowed for the equivalent of a large number of comprehensive tests while maintaining high efficiency, speed, and cost-effectiveness [19]. For each of the three activation modes (physical, chemical, and microwave activation), four factors and three different levels were selected. The $L_9(3^4)$ orthogonal table design test was used. The design factors and levels for physical, chemical, and microwave activation are listed in Tables 1, 2, and 3, respectively. By synthesizing various factors and levels based on the data obtained from the orthogonal test table of the three activation modes (see supplementary data), the optimal preparation conditions for activated carbon could be determined. The orthogonal experiment design focused on analyzing the adsorption properties of activated carbon at different levels and factors, primarily using iodine and methylene blue adsorption values. The analysis methods employed in the orthogonal experiment design included intuitive analysis and variance analysis. Intuitive analysis encompassed range analysis, primary and secondary analysis, and the selection of the optimal scheme. ANOVA was used to determine the significance of each influencing factor. Range analysis involved calculating the average of the levels of each test factor, with range representing the difference between the maximum and minimum averages. The primary and secondary order was determined based on the results of the range analysis, with higher average values indicating better test levels.

2.4 Material characterization and adsorption performance

Through an orthogonal test, the char characteristics of optimum activated carbon obtained by physical, chemical,

Table 1 Levels of physical activation and design factors

Levels	Factors			
	A	B	C	D
	Heating rate (℃/min)	Peanut shell content (%)	Activation temperature (℃)	Activation time (min)
1	10	10	700	30
2	20	20	800	60
3	30	30	900	90

Table 2 Levels of chemical activation and design factors

Levels	Factors			
	A	B	C	D
	Impregnation ratio (mixture-to-zinc chloride)	Peanut shell content (%)	Activation temperature (℃)	Activation time (min)
1	1:2	10	500	30
2	1:2.5	20	550	60
3	1:3	30	600	90

Table 3 Levels of microwave activation and design factors

Levels	Factors			
	A	B	C	D
	Peanut shell content (%)	Microwave power (W)	Impregnation ratio (mixture-to-zinc chloride)	Activation time (min)
1	10	300	1:2	10
2	20	500	1:2.5	20
3	30	700	1:3	30

Table 4 Specific surface area and pore structure parameters of activated carbon

Samples	Specific surface area (m^2/g)	V_{total} (mL/g)	Average pore size (nm)
AC-Raw	224.82	0.21	8.60
AC-P_{max}	453.70	0.65	14.10
AC-C_{max}	803.48	0.59	16.14
AC-M_{max}	401.16	0.47	14.10

and microwave activation were characterized. In order to obtain the specific surface area and other parameters, the activated carbon was determined by an automatic gas adsorption analyzer (Autosorb-IQ, Quantachrome, USA). The surface morphology of activated carbon was observed by scanning electron microscope (Quanta 200, FEI Corporation, USA). The crystal structure of activated carbon was studied using a combined multifunctional horizontal X-ray diffractometer (Ultima IV, Rigaku, Japan). Infrared spectroscopy (Nicolet iS10, Thermo Fisher, USA) was used to characterize the functional group changes on the surface of activated carbon.

In the orthogonal experimental design, the adsorption properties of activated carbon were primarily evaluated based on the adsorption values of iodine and methylene blue. The iodine adsorption value of activated carbon was determined according to the China national standard GB/T12496.8–2015. The methylene blue adsorption capacity of activated carbon was determined according to the China national standard GB/T 12496.10–1999. The literature [20] provided specific procedures for the adsorption of iodine and methylene blue by activated carbon, which could be referred to.

3 Results and discussion

3.1 Activated carbon adsorption experiment

The results of the orthogonal adsorption of iodine and methylene blue on activated carbon, prepared using three different

activation methods (physical, chemical, and microwave activation), are presented in Table S1-S6 in the supplementary data. When compared to AC-Raw (with iodine and methylene blue adsorption capacities of 310 mg/g and 50 mg/g, respectively), the activated carbon prepared by physical activation exhibited average adsorption capacities of 577.2 mg/g for iodine and 107 mg/g for methylene blue. For activated carbon prepared by chemical activation, the average adsorption capacities were 682.5 mg/g for iodine and 121.5 mg/g for methylene blue. Activated carbon prepared by microwave activation showed average adsorption capacities of 503.1 mg/g for iodine and 96.5 mg/g for methylene blue. These results indicated that the adsorption performance of activated carbon prepared by the chemical activation was the highest, followed by the physical activation and finally the microwave activation. Although microwave activation had the advantage of significantly shortening production time, improving production efficiency, and reducing environmental pollution [21], it was not as effective as the physical and chemical activation in improving the adsorption performance of activated carbon. This was likely because the chemical activation was more conducive to the formation of micropores and mesopores. Once inside the micropores, iodine molecules underwent strong physical adsorption with the micropore walls and also underwent substitution reactions with carbonyl or hydroxyl groups on the surface of activated carbon [22]. The presence of mesopores provided a pathway for methylene blue to enter, further enhancing the adsorption performance [23]. The physical activation method used CO_2 reaming to obtain the main mesoporous and macropores [24], resulting in the largest V_{total}, as shown in Table 4. Moreover, Table 4 indicates that compared to physical and microwave activation, the activated

carbon produced through chemical activation had a higher specific surface area of 803.48 m²/g, which promoted better adsorption of iodine and methylene blue. Additionally, the total pore volume of AC-P$_{max}$, AC-C$_{max}$, and AC-M$_{max}$ was 2.2–3.1 times higher than that of AC-Raw, and the average pore size was also increased by 1.6–1.9 times.

Figure 1 illustrates the orthogonal range analysis of the adsorption of iodine and methylene blue by activated carbon under three activation modes (physical, chemical, and microwave activation) by different factors (A, B, C, and D). The values presented in Fig. 1 correspond to the *R* values in the orthogonal test table. Specifically, Fig. 1(a), (c), and (e) depicts the iodine adsorption capacity of activated carbon prepared through physical activation, chemical activation, and microwave activation, respectively. Similarly, Fig. 1(b), (d), and (f) demonstrates the methylene blue adsorption capacity of activated carbon prepared through physical activation, chemical activation, and microwave activation, respectively. In Fig. 1(a) to (f), A, B, C, and D corresponded to the factors listed in Tables 1, 2, and 3. The results shown in Fig. 1(a) and (b) indicate that the peanut shell content (factor B) was the primary factor influencing the adsorption capacity in the physical activation method. In the chemical activation method (Fig. 1(c) and (d)), the activation temperature (factor C) played a crucial role in the iodine adsorption capacity, while the peanut shell content (factor B) had the greatest impact on methylene blue adsorption. In the microwave activation method (Fig. 1(e)

and (f)), the microwave power (factor B) was found to be the main factor affecting the adsorption capacity. The peanut shell content was found to be significant in both physical and chemical activation methods. This was because the addition of peanut shells to the sludge improved the porosity of the activated carbon and increased the number of oxygen-containing functional groups, which facilitated the preparation of high-performance carbon materials. This finding aligned with the conclusion of Liang et al. regarding the co-pyrolysis of coconut shells and sludge for activated carbon production [13]. In terms of the impact of activation time, Zhao et al. discovered, through orthogonal experiment results of coal-based activated carbon, that activation time had the greatest influence on the iodine value of activated carbon [25]. This was primarily due to the fact that a longer activation time led to a higher specific surface area. Similarly, higher microwave power resulted in increased energy input to the activated sample, leading to the formation of more active sites and pores, thus enhancing the adsorption capacity [26]. However, it is important to note that excessive microwave power could cause the activated carbon to burn and damage the pore structure [27].

Through orthogonal test analysis (see supplementary data for specific comparison process), the optimal process parameters and adsorption values for iodine and methylene blue were obtained for three different methods: (1) physical activation method: the heating rate was 20 ℃/min, the peanut shell content was 30%, the activation temperature

Fig. 1 Orthogonal range analysis of adsorption of iodine and methylene blue by activated carbon with different factors (**A**, **B**, **C**, and **D**) in three activation modes (physical activation, chemical activation, and microwave activation)
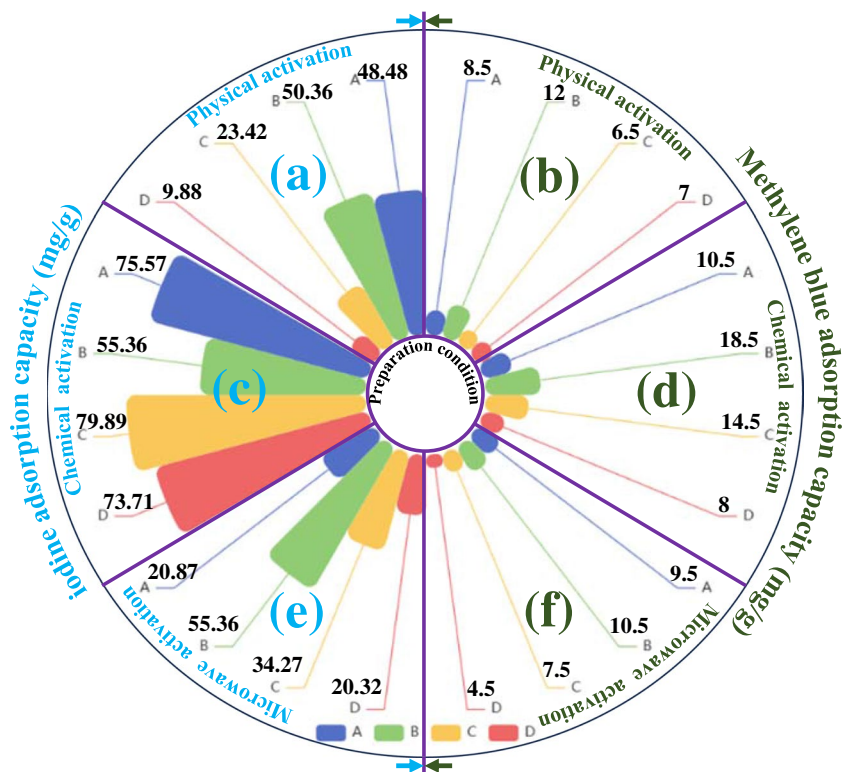
was 800 ℃, and the activation time was 30 min, resulting in an iodine adsorption value of 686.68 mg/g and a methylene blue adsorption capacity of 138 mg/g. (2) Chemical activation method: the impregnation ratio was 1:2, peanut shell content was 30%, activation temperature was 500 °C, and activation time was 30 min, resulting in an iodine adsorption value of 913.86 mg/g and a methylene blue adsorption capacity of 153 mg/g. (3) Microwave activation method: the peanut shell content was 30%, microwave power was 700 W, impregnation ratio was 1:2.5, and activation time was 10 min, resulting in an iodine adsorption value of 607.67 mg/g and a methylene blue adsorption capacity of 118.5 mg/g. In summary, the chemical activation method showed significant advantages over physical activation and microwave activation in terms of preparing activated carbon with high adsorption properties.

3.2 Characterization of activated carbon

Based on the orthogonal test results, BET, SEM, XRD, and FTIR tests were carried out on the activated carbon samples (AC-P$_{max}$, AC-C$_{max}$, and AC-M$_{max}$) prepared under optimized conditions by physical activation, chemical activation, and microwave activation, respectively. In order to understand the char characteristics of the optimal activated carbon, activated carbon (AC-Raw) was selected for comparison.

Figure 2a shows the nitrogen adsorption–desorption isotherm of ACs. The results of Fig. 2a demonstrate that the adsorption–desorption curves of ACs followed typical type IV isotherms at a relative pressure of 0.4–0.9, with the exception of the chemical activation method not being clearly evident. This was attributed to the presence of mesoporous pores, which resulted in capillary condensation during the mesoporous adsorption process at high pressure, leading to the formation of a hysteresis ring [28, 29]. The pore size distribution of ACs is illustrated in Fig. S1, which clearly shows that the primary pore structure of ACs consisted of mesopores, and the pore size distribution was broad, aligning with the average pore size results presented in Table 4.

The surface microscopic appearance of ACs is shown in Fig. 2b. It was evident that the surface morphology
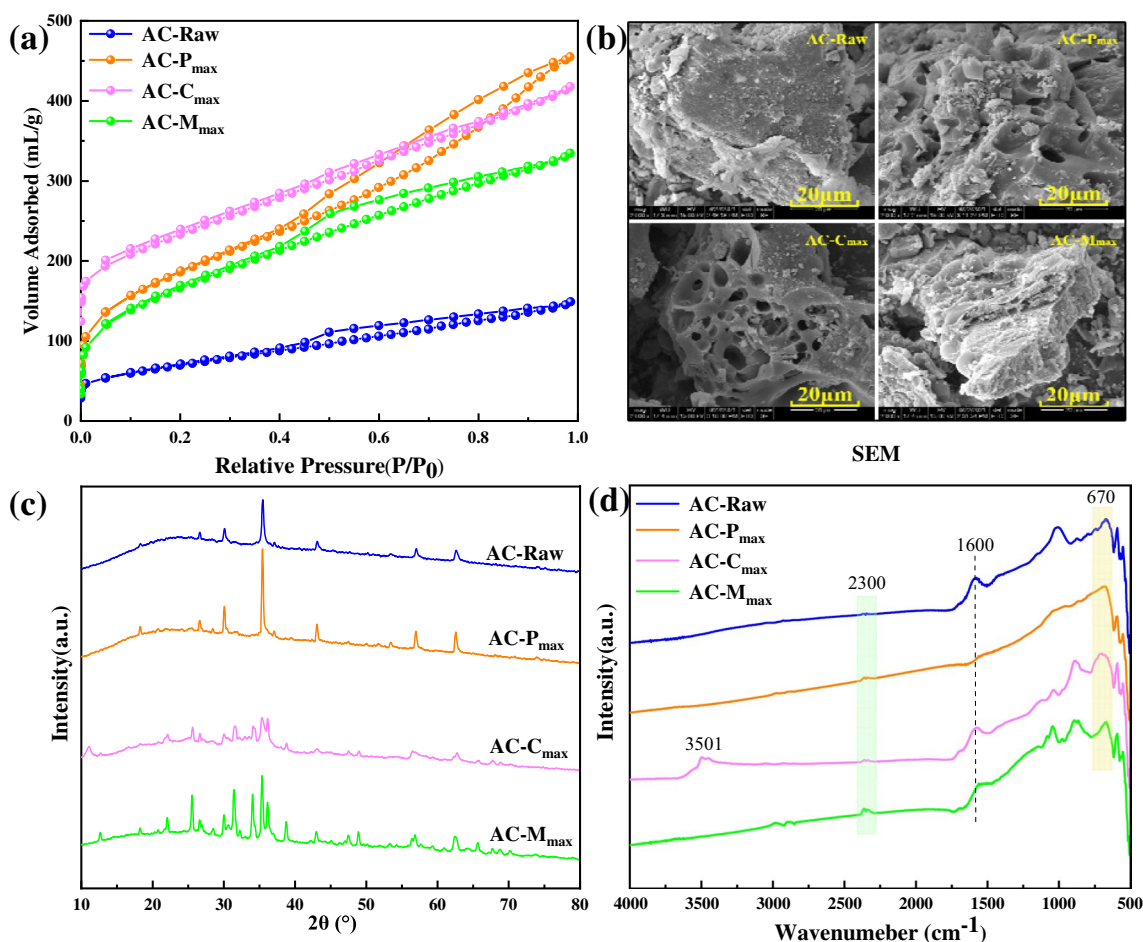

Fig. 2 Characterization of ACs: **a** N$_2$ adsorption–desorption isotherms; **b** SEM images; **c** XRD pattern; **d** FTIR spectra analysis

of AC-Raw was rough, with pores mainly formed due to volatile precipitation during the pyrolysis process. This suggested that the activation achieved through the direct carbonization method was insufficient. On the other hand, AC-P$_{max}$ exhibited CO_2-etched pores on its surface after activation, indicating that the use of high-purity CO_2 as a gas activator had a positive impact on the activated carbon. Furthermore, after chemical activation, AC-C$_{max}$ displayed an abundant pore structure on its surface. This could be attributed to the significant infiltration of $ZnCl_2$ into the feedstock, which acted as a de-hydroxylation and dehydration agent during the activation process. Pimentel et al. found that $ZnCl_2$, a Lewis acid, promoted the production of large-ring aromatic compounds, leading to the formation of uniform micropores [30]. $ZnCl_2$ molecules acted as a support within the carbon structure and evaporated at high temperatures, contributing to the pore size. Washing $ZnCl_2$ resulted in the formation of a porous structure, while some $ZnCl_2$ on the surface eroded the surface, creating pore structures during activation. Xia et al. also observed irregular cracks on the surface of cotton textile waste after $ZnCl_2$ activation, which was attributed to $ZnCl_2$ evaporation during pyrolysis [31]. Microwave activation resulted in minimal pore and crack formation on the surface of AC-M$_{max}$, indicating a limited activation effect.

Figure 2c presents the XRD pattern of the ACs, revealing a diffraction peak at a 2θ value of 36.5°, which was attributed to the characteristic diffraction peak of the quartz phase. Referring to the standard card, it could be concluded that this characteristic peak corresponded to the crystal surface (111), suggesting the presence of Si (in the form of quartz phase) in the carbon-based structure of the carbonization and activation products obtained from the feedstocks. Moreover, the number and intensity of diffraction peaks in the spectra of AC-P$_{max}$, AC-C$_{max}$, and AC-M$_{max}$ were higher than AC-Raw, indicating an enhanced degree of graphitization in the activated carbon after activation.

The infrared spectrum of ACs is presented in Fig. 2d. The infrared spectra of activated carbon prepared using different activation methods exhibited variations. The absorption peak at 3501 cm^{-1} in AC-C$_{max}$ was attributed to the presence of –OH and Si–OH groups in the organic matter [32]. AC-Raw, AC-C$_{max}$, and AC-M$_{max}$ showed distinct peaks around 1600 cm^{-1}, primarily associated with the stretching vibration of –CN. All ACs displayed minor absorption peaks around 2300 cm^{-1}, which were caused by the stretching vibration of alkynes. The absorption peak near 670 cm^{-1} indicated the presence of Si–O–C, Si–O–Si, or C–O–C structures, which were primarily influenced by the significant amount of silicon present in the sludge [33, 34].

3.3 Methyl orange adsorption by optimum activated carbon (AC-C$_{max}$)

The study used chemically activated optimum activated carbon (AC-C$_{max}$) with a higher specific surface area, developed pore size structure, and stable physicochemical properties to investigate its adsorption effect on methyl orange. The effects of adsorption time, activated carbon dose, initial concentration of methyl orange, and pH value of the solution on the adsorption were investigated.

3.3.1 Adsorption property

The adsorption properties were determined by the adsorption capacity (Q) and removal efficiency of methyl orange solution on activated carbon. As shown in the following formula:
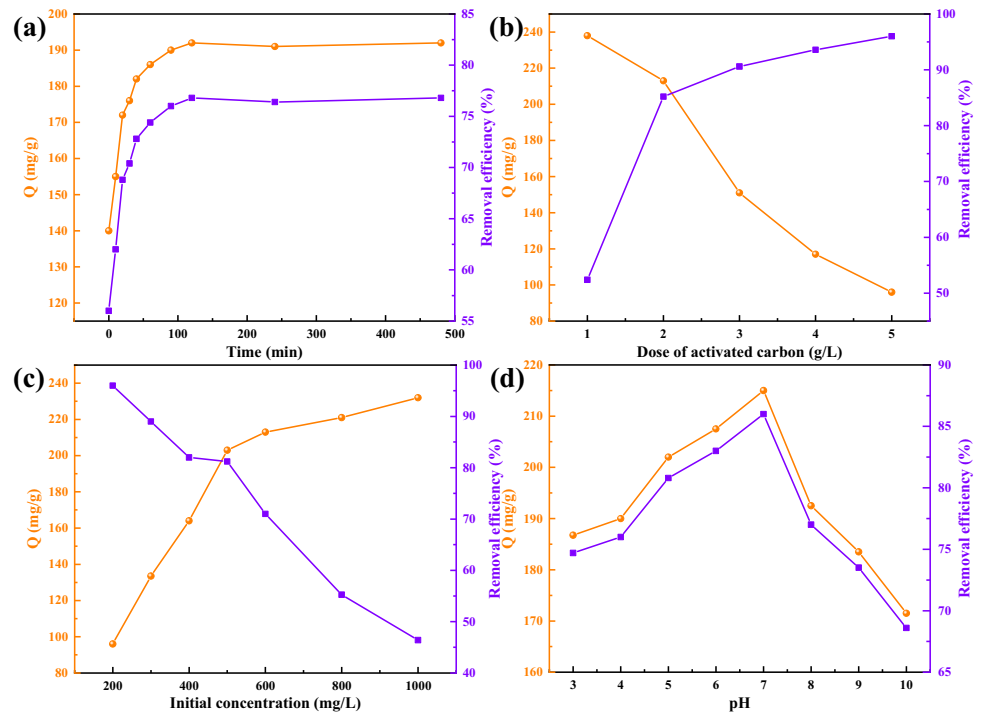
$$Q = \frac{(C_0 - C_e)V}{M} \tag{1}$$

$$R = \frac{(C_0 - C_e)}{C_0} \times 100\% \tag{2}$$

where Q is the adsorption capacity of activated carbon (mg/g), R is the removal efficiency of methyl orange by activated carbon (%), C_0 is the initial concentration of methyl orange solution (mg/L), C_e is the concentration of methyl orange solution after adsorption (mg/L), V is the volume of solution (L), and M is the mass of activated carbon (g).

A 25 mL solution of methyl orange with an initial concentration of 500 mg/L was prepared. The pH value of the solution was adjusted to 7, and 0.05 g of AC-C$_{max}$ was added. The effect of activated carbon on the adsorption of methyl orange was studied at 25 ℃ for different adsorption times (5, 15, 30, 45, 60, 90, 120, 240, and 480 min), and the results are presented in Fig. 3a. The adsorption capacity and removal efficiency of methyl orange solution remained consistent as the adsorption time increased. Initially, the adsorption capacity and removal efficiency of activated carbon increased rapidly within the first 90 min and then gradually stabilized. After 120 min, the adsorption process reached equilibrium. Therefore, the entire adsorption process could be divided into three stages: fast, slow, and dynamic equilibrium. The adsorption equilibrium time for subsequent tests was determined to be 120 min. Initially, the sludge-based activated carbon had numerous vacant adsorption points on its surface. As time progressed and the adsorption reaction took place, methyl orange molecules occupied a significant number of adsorption sites on the activated carbon surface and gradually penetrated into its interior [35]. This resulted in a decrease in the mass transfer rate, affecting

Fig. 3 The effect of optimal activated carbon on the adsorption capacity (Q) and removal efficiency of methyl orange under different factors: **a** adsorption time; **b** activated carbon dose; **c** initial concentration; **d** pH value

the adsorption rate and amount. When dynamic equilibrium was reached, the maximum adsorption capacity of activated carbon for methyl orange solution was found to be 192 mg/g, with a maximum removal rate of 76.8%.

Figure 3b illustrates the impact of adding different amounts of activated carbon (1 g/L, 2 g/L, 3 g/L, 4 g/L, and 5 g/L) on the adsorption performance of methyl orange solution at 25 ℃ for 120 min. As the dose of activated carbon increased, the removal efficiency of methyl orange solution noticeably improved, while the adsorption capacity exhibited a downward trend. The increase in activated carbon dose led to an increase in the surface area and surface active groups, which enhanced the removal efficiency of methyl orange [36]. However, the amount of methyl orange adsorbed by activated carbon gradually decreased during this process. This could be attributed to the competition for adsorption sites between methyl orange molecules in the solution when the amount of carbon added was lower than the concentration of methyl orange solution, resulting in a large adsorption amount. As the activated carbon dose increased, the relative concentration of carbon in the solution increased, causing particle condensation and reducing the surface area available for effective carbon adsorption. This, in turn, decreased the number of effective adsorption sites and increased the diffusion distance of methyl orange molecules on the surface and inside of the carbon, ultimately leading to a decrease in the adsorption amount [37]. Considering the adsorption capacity, removal efficiency, and economy, a dose of 2 g/L of activated carbon was chosen for subsequent tests.

When the activated carbon was 0.05 g and the adsorption time was 2 h at 25 ℃, the effects of different initial concentrations of methyl orange solution on the adsorption properties of activated carbon were investigated (Fig. 3c). The initial concentrations tested were 200 mg/L, 300 mg/L, 400 mg/L, 500 mg/L, 600 mg/L, 800 mg/L, and 1000 mg/L. It was observed that the adsorption capacity of methyl orange by activated carbon increased rapidly when the initial concentration of the solution was in the range of 200 to 500 mg/L. This could be attributed to the low concentration of methyl orange solution, which was not sufficient to occupy all the adsorption sites on activated carbon. As a result, there was a significant collision contact between methyl orange molecules and activated carbon, allowing for full adsorption. Additionally, the concentration difference between the solid and liquid phases increased the propagation rate of methyl orange molecules, leading to a reduction in transfer resistance. However, with the increase in solution concentration, the number of available adsorption sites on activated carbon gradually decreased. Liu et al. also suggested that the increase in initial concentration provided a driving force to overcome the transfer resistance, thereby enhancing the adsorption capacity of activated carbon [38]. Nevertheless, as the active sites on activated carbon approached saturation at higher concentrations, the adsorption capacity tended to stabilize. Consequently, the adsorption capacity of methyl orange by activated carbon initially increased rapidly and then slowed down steadily, while the removal efficiency showed a downward trend. When the

solution concentration reached 500 mg/L, the adsorption capacity of activated carbon gradually reached saturation.

The pH value of the solution had an impact on the surface charge of activated carbon and the form of methyl orange, which in turn affected the adsorption performance of activated carbon. In the experiment, when 0.05 g of activated carbon was used, the adsorption time was 2 h at 25 ℃, and the concentration of the methyl orange solution was 500 mg/L. Figure 3d illustrates the influence of different pH values (3, 4, 5, 6, 7, 8, 9, 10) on the adsorption of methyl orange solution by activated carbon. Under acidic conditions, the presence of a large amount of H$^+$ in the solution could neutralize the negatively charged active sites on the slightly alkaline surface of methyl orange, thereby hindering the cross-linking between the active sites of methyl orange and activated carbon. As the pH value of the solution continued to rise, the degree of neutralization decreased, allowing the pore structure of activated carbon to continuously adsorb the active sites of methyl orange. Consequently, the removal efficiency and adsorption capacity of methyl orange continued to increase. The highest removal efficiency and adsorption capacity of methyl orange, reaching 86.37% and 215.93 mg/g respectively, were achieved at a pH value of 7. As the pH value of the solution further increased, the surface of activated carbon became negatively charged, leading to electrostatic repulsion with the negatively charged methyl orange under alkaline conditions. Consequently, the adsorption capacity and removal efficiency of activated carbon on methyl orange decreased significantly.

3.3.2 Adsorption kinetics

Adsorption kinetics refers to the change in reaction rate over time during a chemical reaction. In the study of adsorption kinetics of methyl orange, both quasi-first-order and quasi-second-order kinetic models were employed. The quasi-first-order kinetic model describes the adsorption rate based on the adsorption amount. According to this model, the unadsorbed point is directly proportional to the adsorption

rate, and the adsorption process is controlled by the diffusion step. The quasi-first-order kinetic equation for adsorption can be expressed as follows:

$$q_t = q_{e1}(1 - e^{-k_1 t}) \tag{3}$$

The quasi-second-order kinetic model assumes that the rate at which adsorbents occupy active sites on activated carbon is proportional to the square of the number of unoccupied active sites. The quasi-second-order adsorption kinetic equation is expressed as follows:

$$\frac{t}{q_t} = \frac{1}{k_2 q_{e2}^2} + \frac{1}{q_{e2}}t \tag{4}$$

where q_t is the adsorption capacity of methyl orange by activated carbon at time t (mg/g), q_{e1} and q_{e2} are theoretical equilibrium adsorption capacity (mg/g), k_1 is the quasi-first-order adsorption kinetic constant, and k_2 is the quasi-second-order adsorption kinetic constant.

According to Eqs. (3) and (4), the data were fitted and calculated, and the results are presented in Fig. 4a and b. The parameters of the calculated quasi-first-order equation and quasi-second-order equation are summarized in Table 5. It was found that Lagergren's quasi-second-order kinetic model provided a better description of the adsorption behavior of methyl orange on activated carbon compared to the quasi-first-order kinetic model. The correlation coefficient R^2 was greater than 0.999, indicating a strong relationship. Furthermore, the equilibrium adsorption amount calculated by the quasi-second-order adsorption kinetics model

Table 5 Adsorption kinetics model fitting results and parameter values

Quasi-first-order kinetic model			Quasi-second-order kinetic model		
q_{e1} (mg/g)	k_1	R_1^2	q_{e2} (mg/g)	k_2	R_2^2
181.78	1.4704	0.96106	192.68	0.0028	0.99970

Fig. 4 Lagergren dynamics fitting: **a** quasi-first-order equation; **b** quasi-second-order equation
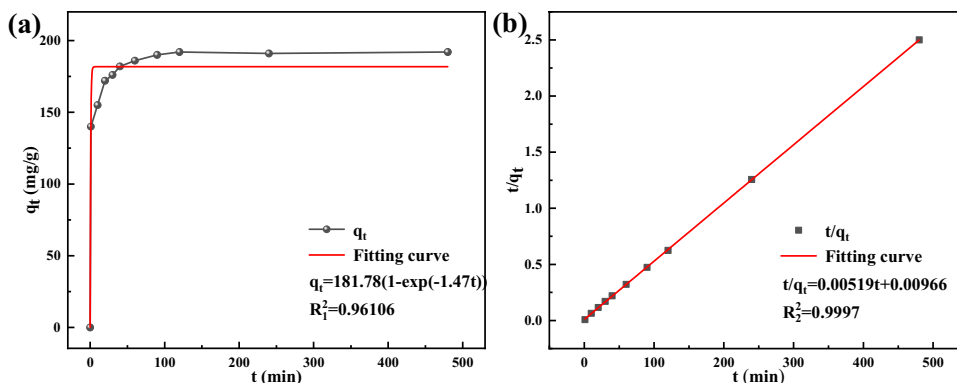
closely matched the actual value, suggesting the occurrence of chemical bond formation during the chemical adsorption of methyl orange by the optimal activated carbon [39].

The adsorption process of adsorbates on the adsorbent is generally more complex and can be divided into two stages: the first stage involves the transfer of adsorbates to the surface of the adsorbent particles, known as external diffusion, and the second stage involves the transfer of adsorbates from the surface of the adsorbent to the pores inside the particles, known as internal diffusion. In order to provide a better understanding of the adsorption process, researchers have developed intraparticle diffusion models [40]. The formula is as follows:

$$q_t = k_p t^{0.5} + C \qquad (5)$$

where k_p is the intraparticle diffusion constant (mg/g·min^{-1}), C is a constant related to the thickness of the boundary layer, and q_t is the amount of methyl orange adsorbed by activated carbon at time t (mg/g).

Table 6 shows that the adsorption of methyl orange by activated carbon has a strong fitting effect in the external diffusion stage, with $R^2 > 0.99$. However, the fitting effect in the internal diffusion stage was poor, and the linear relationship was not observed. These results suggested that the adsorption rate of methyl orange was not solely determined by the intraparticle diffusion process. The overall adsorption process was also influenced by factors such as the concentration of adsorbates, affinity, pore size, and distribution of the adsorbent [41]. Furthermore, comparing the k_p values of the two diffusion stages revealed that the movement speed of adsorbates from the external diffusion stage to the particle surface was higher than that from the adsorbent surface to the particle pores in the internal diffusion stage.

4 Conclusions

In this study, an orthogonal test was conducted to screen activated carbon treated by physical activation, chemical activation, and microwave activation, in order to obtain the optimal activated carbon. The surface morphology and physicochemical properties of the optimal activated

carbon were analyzed, and its application in the adsorption of methyl orange was investigated. Based on the above discussion, the following conclusions can be drawn:

- Through the orthogonal test, it was found that AC-C$_{max}$ prepared by chemical activation outperformed the activated carbon prepared by physical and microwave activation. The iodine adsorption value of AC-C$_{max}$ was measured to be 913.86 mg/g, while the methylene blue adsorption value was found to be 153 mg/g. The optimal chemical activation conditions for AC-C$_{max}$ were determined to be an impregnation ratio of 1:2, peanut shell content of 30%, activation temperature of 500 °C, and activation time of 30 min.
- According to BET and SEM analysis, AC-C$_{max}$ exhibited a higher specific surface area and a more developed pore structure. XRD analysis indicated that Si was present in the carbon-based structure as a quartz phase in both the carbonization and activation products of feedstocks, with the activated samples showing a higher degree of graphitization. FTIR analysis revealed an increased presence of oxygen-containing functional groups on the surface of AC-C$_{max}$.
- The adsorption equilibrium time of AC-C$_{max}$ for methyl orange solution was found to be 120 min. As the activated carbon dose increased, the removal efficiency of methyl orange noticeably improved, while the adsorption capacity decreased. Similarly, the adsorption capacity of AC-C$_{max}$ on methyl orange increased with an increase in the initial concentration. However, it was observed that the adsorption capacity gradually reached saturation when the initial concentration reached 500 mg/L. At a pH value of 7, the highest removal efficiency and adsorption capacity of methyl orange were achieved, with values of 86.37% and 215.93 mg/g, respectively.
- The adsorption kinetics of methyl orange by AC-C$_{max}$ was better described by the quasi-second-order kinetic equation, with $R^2 > 0.999$. The fit of AC-C$_{max}$ adsorption of methyl orange in the external diffusion stage was highly accurate, but the fit in the internal diffusion stage is poor, suggesting that internal diffusion did not play a significant role in controlling the adsorption process.

Table 6 Model parameters of intraparticle diffusion of methyl orange by activated carbon

External diffusion stage			Internal diffusion stage		
k_{pE} (mg/g)	C_E	R_E^2	k_{pI} (mg/g)	C_I	R_I^2
7.2125	134.623	0.996	0.28631	186.444	0.755

The subscripts E and I indicate the external and internal diffusion stages, respectively

Declarations

Ethical approval Not applicable.

Consent to participate Not applicable.

Consent for publication Not applicable.

Competing interests The authors declare no competing interests.

References

1. Hadi P, Xu M, Ning C, Sze Ki Lin C, McKay G (2015) A critical review on preparation, characterization and utilization of sludge-derived activated carbons for wastewater treatment. Chem Eng J 260:895–906. https://doi.org/10.1016/j.cej.2014.08.088

2. Bjorklund K, Li LY (2017) Adsorption of organic stormwater pollutants onto activated carbon from sewage sludge. J Environ Manage 197:490–497. https://doi.org/10.1016/j.jenvman.2017.04.011

3. China Paper Association (2023) China paper industry 2022 annual report. China Pulp & Paper Industry. 44: 21–30+6. https://kns.cnki.net/kcms2/article/abstract?v=0kbmF0AymBCYyQN8as5Nacen2GJkvOjEzbmOiQwQS_rS9UOd7EFxtXsCLXtc19Qgatawr5pngHsZbRxYmamVlS5Q3OMl9jSR8OWKCKNltdb52m9iMWh9BXLxh7PrBp1V1m5gCZjcSWzw3c6uuKUFFA==&uniplatform=NZKPT&language=CHS

4. Priadi C, Wulandari D, Rahmatika I, Moersidik SS (2014) Biogas production in the anaerobic digestion of paper sludge. APCBEE Proc 9:65–69. https://doi.org/10.1016/j.apcbee.2014.01.012

5. Cheng F, Luo H, Hu L, Yu B, Luo Z, Fidalgo de Cortalezzi M (2016) Sludge carbonization and activation: from hazardous waste to functional materials for water treatment. J Environ Chem Eng 4(4):4574–4586. https://doi.org/10.1016/j.jece.2016.11.013

6. Gao Y, Gao W, Zhu H, Chen H, Yan S, Zhao M, Sun H, Zhang J, Zhang S (2022) A review on n-doped biochar for oxidative degradation of organic contaminants in wastewater by persulfate activation. Int J Environ Res Public Health 19(22):14805. https://doi.org/10.3390/ijerph192214805

7. Ewuzie U, Saliu OD, Dulta K, Ogunniyi S, Bajeh AO, Iwuozor KO, Ighalo JO (2022) A review on treatment technologies for printing and dyeing wastewater (PDW). J Water Process Eng 50:103273. https://doi.org/10.1016/j.jwpe.2022.103273

8. Li Y, Li Y, Li L, Shi X, Wang Z (2016) Preparation and analysis of activated carbon from sewage sludge and corn stalk. Adv Powder Technol 27(2):684–691. https://doi.org/10.1016/j.apt.2016.02.029

9. Zaker A, Chen Z, Wang X, Zhang Q (2019) Microwave-assisted pyrolysis of sewage sludge: a review. Fuel Process Technol 187:84–104. https://doi.org/10.1016/j.fuproc.2018.12.011

10. Agrafioti E, Bouras G, Kalderis D, Diamadopoulos E (2013) Biochar production by sewage sludge pyrolysis. J Anal Appl Pyrolysis 101:72–78. https://doi.org/10.1016/j.jaap.2013.02.010

11. Yang B, Liu Y, Liang Q, Chen M, Ma L, Li L, Liu Q, Tu W, Lan D, Chen Y (2019) Evaluation of activated carbon synthesized by one-stage and two-stage co-pyrolysis from sludge and coconut shell. Ecotoxicol Environ Saf 170:722–731. https://doi.org/10.1016/j.ecoenv.2018.11.130

12. Wang AY, Sun K, Wu L, Wu P, Zeng W, Tian Z, Huang QX (2020) Co-carbonization of biomass and oily sludge to prepare sulfamethoxazole super-adsorbent materials. Sci Total Environ 698:134238. https://doi.org/10.1016/j.scitotenv.2019.134238

13. Liang Q, Liu Y, Chen M, Ma L, Yang B, Li L, Liu Q (2020) Optimized preparation of activated carbon from coconut shell and municipal sludge. Mater Chem Phys 241:122327. https://doi.org/10.1016/j.matchemphys.2019.122327

14. Nielsen L, Zhang P, Bandosz TJ (2015) Adsorption of carbamazepine on sludge/fish waste derived adsorbents: effect of surface chemistry and texture. Chem Eng J 267:170–181. https://doi.org/10.1016/j.cej.2014.12.113

15. dos Reis GS, Wilhelm M, Silva TCDA, Rezwan K, Sampaio CH, Lima EC, de Souza SMAGU (2016) The use of design of experiments for the evaluation of the production of surface rich activated carbon from sewage sludge via microwave and conventional pyrolysis. Appl Therm Eng 93:590–597. https://doi.org/10.1016/j.applthermaleng.2015.09.035

16. Tay JH, Chen XG, Jeyaseelan S, Graham N (2001) Optimising the preparation of activated carbon from digested sewage sludge and coconut husk. Chemosphere 44(1):45–51. https://doi.org/10.1016/s0045-6535(00)00383-0

17. Gayathiri M, Pulingam T, Lee KT, Sudesh K (2022) Activated carbon from biomass waste precursors: factors affecting production and adsorption mechanism. Chemosphere 294:133764. https://doi.org/10.1016/j.chemosphere.2022.133764

18. Yang J, Qiu K (2010) Preparation of activated carbons from walnut shells via vacuum chemical activation and their application for methylene blue removal. Chem Eng J 165(1):209–217. https://doi.org/10.1016/j.cej.2010.09.019

19. Zhong L, Zhang Y, Wang T, Ji Y, Norris P, Pan W-P (2018) Optimized methods for preparing activated carbon from rock asphalt using orthogonal experimental design. J Therm Anal Calorim 136(5):1989–1999. https://doi.org/10.1007/s10973-018-7855-x

20. Wu H, Dong Z, Sun J, Ding K (2023) Boosting the adsorption capacity of activated carbon prepared from Amygdalus communis shells using physicochemical co-activation method. Biomass Convers Biorefin. https://doi.org/10.1007/s13399-023-04093-0

21. Ahmed MJ (2016) Application of agricultural based activated carbons by microwave and conventional activations for basic dye adsorption: review. J Environ Chem Eng 4(1):89–99. https://doi.org/10.1016/j.jece.2015.10.027

22. Ho K, Chun H, Lee HC, Lee Y, Lee S, Jung H, Han B, Lee C-H (2019) Design of highly efficient adsorbents for removal of gaseous methyl iodide using tertiary amine-impregnated activated carbon: Integrated experimental and first-principles approach. Chem Eng J 373:1003–1011. https://doi.org/10.1016/j.cej.2019.05.115

23. Huang Y, Cannon FS, Guo J, Watson JK, Mathews JP (2016) Atomistic modelling insight into the structure of lignite-based activated carbon and benzene sorption behavior. RSC Adv 6(61):56623–56637. https://doi.org/10.1039/c6ra07533a

24. Barczak B, Łuczak J, Kazimierski P, Klugmann-Radziemska E, Lopez G, Januszewicz K (2023) Exploring synergistic effects in physical-chemical activation of Acorus calamus for water treatment solutions. J Environ Manage 347:119000. https://doi.org/10.1016/j.jenvman.2023.119000

25. Zhao C, Ge L, Mai L, Chen S, Li Q, Yao L, Li D, Wang Y, Xu C (2023) Preparation and performance of coal-based activated carbon based on an orthogonal experimental study. Energy 274:127353. https://doi.org/10.1016/j.energy.2023.127353

26. Ao W, Fu J, Mao X, Kang Q, Ran C, Liu Y, Zhang H, Gao Z, Li J, Liu G, Dai J (2018) Microwave assisted preparation of activated carbon from biomass: a review. Renew Sustain Energy Rev 92:958–979. https://doi.org/10.1016/j.rser.2018.04.051

27. Foo KY, Hameed BH (2012) Coconut husk derived activated carbon via microwave induced activation: effects of activation agents,

preparation parameters and adsorption performance. Chem Eng J 184:57–65. https://doi.org/10.1016/j.cej.2011.12.084

28. Yu M, Li J, Wang L (2016) Preparation and characterization of magnetic carbon aerogel from pyrolysis of sodium carboxymethyl cellulose aerogel crosslinked by iron trichloride. J Porous Mater 23(4):997–1003. https://doi.org/10.1007/s10934-016-0157-4

29. Tran HN, You S-J, Chao H-P (2017) Fast and efficient adsorption of methylene green 5 on activated carbon prepared from new chemical activation method. J Environ Manage 188:322–336. https://doi.org/10.1016/j.jenvman.2016.12.003

30. Pimentel CH, Freire MS, Gómez-Díaz D, González-Álvarez J (2023) Preparation of activated carbon from pine (Pinus radiata) sawdust by chemical activation with zinc chloride for wood dye adsorption. Biomass Convers Biorefin 13:16537–16555. https://doi.org/10.1007/s13399-023-04138-4

31. Xia M, Shao X, Sun Z, Xu Z (2020) Conversion of cotton textile wastes into porous carbons by chemical activation with ZnCl(2), H(3)PO(4), and FeCl(3). Environ Sci Pollut Res 27(20):25186–25196. https://doi.org/10.1007/s11356-020-08873-3

32. Kaçan E, Kütahyalı C (2012) Adsorption of strontium from aqueous solution using activated carbon produced from textile sewage sludges. J Anal Appl Pyrolysis 97:149–157. https://doi.org/10.1016/j.jaap.2012.06.006

33. Gu L, Zhu N, Guo H, Huang S, Lou Z, Yuan H (2013) Adsorption and Fenton-like degradation of naphthalene dye intermediate on sewage sludge derived porous carbon. J Hazard Mater 246–247:145–153. https://doi.org/10.1016/j.jhazmat.2012.12.012

34. Silva TL, Ronix A, Pezoti O, Souza LS, Leandro PKT, Bedin KC, Beltrame KK, Cazetta AL, Almeida VC (2016) Mesoporous activated carbon from industrial laundry sewage sludge: adsorption studies of reactive dye Remazol Brilliant Blue R. Chem Eng J 303:467–476. https://doi.org/10.1016/j.cej.2016.06.009

35. Liu S, Shen C, Wang Y, Huang Y, Hu X, Li B, Karnowo ZJ, Zhang S, Zhang H (2021) Development of CO2/H2O activated biochar derived from pine pyrolysis: application in methylene blue adsorption. J Chem Technol Biotechnol 97(4):885–893. https://doi.org/10.1002/jctb.6971

36. Serban GV, Iancu VI, Dinu C, Tenea A, Vasilache N, Cristea I, Niculescu M, Ionescu I, Chiriac FL (2023) Removal efficiency and adsorption kinetics of methyl orange from wastewater by commercial activated carbon. Sustainability 15(17):12939. https://doi.org/10.3390/su151712939

37. Örnek A, Özacar M, Şengil İA (2007) Adsorption of lead onto formaldehyde or sulphuric acid treated acorn waste: equilibrium and kinetic studies. Biochem Eng J 37(2):192–200. https://doi.org/10.1016/j.bej.2007.04.011

38. Liu Z, Zhang FS (2009) Removal of lead from water using biochars prepared from hydrothermal liquefaction of biomass. J Hazard Mater 167(1–3):933–939. https://doi.org/10.1016/j.jhazmat.2009.01.085

39. Bedin KC, Martins AC, Cazetta AL, Pezoti O, Almeida VC (2016) KOH-activated carbon prepared from sucrose spherical carbon: adsorption equilibrium, kinetic and thermodynamic studies for methylene blue removal. Chem Eng J 286:476–484. https://doi.org/10.1016/j.cej.2015.10.099

40. Wang J, Guo X (2022) Rethinking of the intraparticle diffusion adsorption kinetics model: interpretation, solving methods and applications. Chemosphere 309(2):136732. https://doi.org/10.1016/j.chemosphere.2022.136732

41. Lu J, Zhou Y, Zhou Y (2023) Recent advance in enhanced adsorption of ionic dyes from aqueous solution: a review. Crit Rev Environ Sci Technol 53(19):1709–1730. https://doi.org/10.1080/10643389.2023.2200714